Journal of FISH BIOLOGY
Published for the Fisheries Society of the British Isles

Journal of Fish Biology (2011) **78**, 1799–1823
doi:10.1111/j.1095-8649.2011.02957.x, available online at wileyonlinelibrary.com

Musculoskeletal structure of the feeding system and implications of snout elongation in *Hippocampus reidi* and *Dunckerocampus dactyliophorus*

H. Leysen*†, J. Christiaens*, B. De Kegel*, M. N. Boone‡, L. Van Hoorebeke‡ and D. Adriaens*

**Research Group Evolutionary Morphology of Vertebrates, Ghent University, K.L. Ledeganckstraat 35, B-9000 Gent, Belgium and ‡UGCT, Department of Physics and Astronomy, Proeftuinstraat 86, B-9000 Gent, Belgium*

A thorough morphological description of the feeding apparatus in *Hippocampus reidi*, a long-snouted seahorse, and *Dunckerocampus dactyliophorus*, an extremely long-snouted pipefish, revealed specialized features that might be associated with the fast and powerful suction feeding, like the two ligamentous connections between the lower jaw and the hyoid, the saddle joint of the latter with the suspensorium and the vertebro-pectoral fusion that articulates on three points with the cranium. Despite the conserved morphology of the feeding apparatus, it was found that in *H. reidi* the orientation of the occipital joint is ventrocaudal, the sternohyoideus and epaxial muscles are more bulky and both have a short tendon. In *D. dactyliophorus*, on the other hand, the protractor hyoidei muscle is enclosed by the mandibulo-hyoid ligament, the sternohyoideus and epaxial tendons are long and a sesamoid bone is present in the latter. These features were compared to other syngnathid species with different snout lengths to evaluate the implications of snout elongation on the musculoskeletal structure of the cranium. The arched path of the adductor mandibulae and the greater rigidity of the lower jaw might be related to elongation of the snout, as it yields an increased mechanical advantage of the lower jaw system and a reduced torque between the elements of the lower jaw during protractor hyoidei muscle contraction, respectively. Nevertheless, most observed features did not seem to be related to snout length, but might be associated with different force-generating strategies.

Key words: functional morphology; pipefishes; seahorses; suction feeding.

INTRODUCTION

Pipefishes and seahorses (Syngnathidae) are remarkable animals. The extended body is covered with an armour of bony plates instead of scales, they have independently movable eyes and males have a special reproductive structure, a pouch or a brooding area, whether or not covered by overlapping membranes, to brood the eggs and young (Herald, 1959; Vincent & Sadler, 1995; Lourie *et al.*, 1999; Wilson *et al.*, 2001; Kuiter, 2003; Nelson, 2006). In addition, seahorses (*Hippocampus* sp.) are characterized by a grasping tail instead of a caudal fin, a vertical body axis and a tilted head (Lourie *et al.*, 1999, 2004). The evolution of this upright body posture

†Author to whom correspondence should be addressed. Tel.: +329 264 52 20; email: heleen.leysen@ugent.be

might be related to the late Oligocene expansion of seagrass habitats because the vertical leaves serve as effective camouflage for seahorses, favouring both ambushing prey and avoiding predation (Teske & Beheregaray, 2009). A vertical body position has also been suggested to increase the distance from which a prey can be captured during suction feeding (Van Wassenbergh *et al*., 2011*b*). Besides this, syngnathids have a tubular snout, formed by the elongation of the ethmoid region (Leysen *et al*., 2010). Within the family a large diversity in the snout morphology exists, ranging from very short-snouted species, like softcoral pipefish *Siokunichthys breviceps* Smith 1963, to species with an extremely elongated snout, like weedy seadragon *Phyllopteryx taeniolatus* (Lacépède 1804). All syngnathid species studied thus far are known to perform fast and powerful suction feeding with their snout (Ryer & Orth, 1987; Bergert & Wainwright, 1997; de Lussanet & Muller, 2007; Van Wassenbergh *et al*., 2008; Roos *et al*., 2009*a*; Storero & González, 2009). In teleosts, suction feeding is a common feeding pattern. It involves a fast enlargement of the orobranchial cavity resulting in a pressure difference between the inside of that cavity and the surrounding water. When the jaws open, a water flow is created which will transport the prey into the mouth. The orobranchial expansion can be generated in ventral, dorsal, lateral and rostral directions by hyoid depression, neurocranial elevation, suspensorial abduction and both maxillary protrusion and lower jaw depression, respectively (Lauder, 1983). In pipefishes and seahorses (Syngnathidae), however, the jaws are not protrusible (Branch, 1966; Bergert & Wainwright, 1997) and there is almost no ventral expansion of the buccal cavity by means of hyoid rotation (Roos *et al*., 2009*b*). Instead, the main buccal volume increase in syngnathids is achieved by rapid suspensorial abduction, induced by the retraction of the hyoid and depression of the lower jaw, where neurocranial elevation positions the mouth close to the prey (Roos *et al*., 2009*b*). This type of feeding, where only the head and not the entire body is accelerated towards the prey, is called pivot feeding (de Lussanet & Muller, 2007) and is also found in some deep-sea fishes and flatfishes (Tchernavin, 1953; Muller & Osse, 1984; Gibb, 1995, 1997).

Despite a large variation in the snout morphology between species (Kuiter, 2003), the feeding mechanism of syngnathids seems quite conserved. Hence, what is the optimal morphology, *i.e.* longer or shorter snout, for this specialized type of suction feeding? Kendrick & Hyndes (2005) predicted that syngnathids with longer snouts would be able to attack prey from a greater distance and with greater speed than those with shorter snouts, and thus would be more successful at catching relatively fast-moving prey. Their predictions were confirmed by a dietary analysis of both short- and long-snouted species. Also de Lussanet & Muller (2007) argued that the optimal snout length is a species-specific trade-off between a long snout on one hand, which decreases the angle the head needs to rotate and hence the time to approach the prey, and a short snout on the other, which decreases the moment of inertia of the head resulting in faster prey intake. Van Wassenbergh *et al*. (2011*a*) performed kinematical analyses of prey capture events in both the long-snouted ringed pipefish *Dunckerocampus dactyliophorus* (Bleeker 1853) and the short-snouted bluestripe pipefish *Doryrhamphus melanopleura* (Bleeker 1858). They noted that the total distance travelled by the snout tip during pivot feeding is longer in *D. dactyliophorus*. This suggests that species with a long snout can attack prey from further away, so probably more elusive prey can be caught. On the other hand, short-snouted species showed shorter prey capture times (Van Wassenbergh *et al*., 2011*a*). A more

recent study (Roos *et al*., 2011) shows that a large snout diameter improves volume increase and expansion time, but negatively affects maximal flow velocity. A long snout reduces both maximal flow velocity and suction volume; however, the time to reach the prey is decreased.

Considering the highly specialized feeding strategy of syngnathids, *i.e.* the high-velocity pivot feeding with suspensorium abduction and neurocranial elevation, it can be assumed that this has been associated with adaptive evolutionary modifications in the cranial musculoskeletal system. In addition, more specialized species are generally thought to show a reduced morphological versatility as even the smallest deviation of one element of the complex integrated system can have an effect on the performance (Adriaens & Herrel, 2009). Hence, the hypothesis tested in this study is that the syngnathid trophic apparatus, being highly specialized, will show a conserved morphology to some degree but where existing structural variation can be related to variation in snout length. In addition, as changes in the snout geometry will have an effect on functional lever systems (especially at the level of tendons, ligaments and their attachments), differences are expected to be found that reflect compensations to sustain kinematic v. force efficiency in these lever systems. For example, the elongation of the snout and with it that of the jaw-closing adductor mandibulae muscle complex is expected to be associated with a change in its musculoskeletal architecture. So, an arrangement of the jaw closure apparatus in the longer snouted species to assure the same kinematical efficiency is expected. The mechanical advantage of the lower jaw lever system is for instance increased by increasing the height of the coronoid process of the dentary bone (where the adductor mandibulae tendons attach) or by a more dorsocaudally orientated muscle's line of action with respect to the jaw articulation. In addition, when the protractor hyoidei muscle contracts while the mouth is kept closed, it might induce some torque between the elements of the lower jaw. Long-snouted species probably generate higher strain levels in the muscle and therefore the interdigitation between the anguloarticular and dentary bones is expected to be more firm. Finally, when snout length increases, the moment of inertia during head rotation will increase as well, so a larger power output is needed to accomplish fast neurocranial elevation. This might be realized by a larger epaxial muscle mass or an improved power amplifying system, such as a longer epaxial tendon.

In order to validate these hypotheses, a thorough morphological description of the feeding apparatus in the longsnout seahorse *Hippocampus reidi* Ginsburg 1933 and an extremely long-snouted pipefish *D. dactyliophorus* is given and discussed in relation to other syngnathid species with a large range of snout lengths.

MATERIALS AND METHODS

All animals (Table I) were obtained from commercial trade (Bassleer Biofish; http://www.bassleer.com/; and De Jong Marinelife; http://www.dejongmarinelife.nl/) in accordance with the Convention on International Trade in Endangered Species (CITES) requirements. Specimens were sacrificed by an overdose of MS-222 (tricaine methanesulphonate) and fixed in a 10% buffered and neutralized formalin solution.

DISSECTIONS

For the study of soft tissue structures, such as ligaments, tendons and muscles, dissections were performed on three specimens of *H. reidi*, one specimen of *D. dactyliophorus*, one

TABLE I. List of specimens studied, the number of specimens (n), their standard length (L_S), head length (L_H), head length:snout length (L_{Sn}) ratio (L_H:L_{Sn}) and purpose

Species	n	L_S (mm)	L_H (mm)	L_H:L_{Sn}	Used for
Hippocampus reidi	3	113·7–152·8	23·8–32·2	2·2–2·5	Dissecting
Hippocampus reidi	3	109·7–117·2	21·4–24·4	2·2–2·5	Clearing and staining
Hippocampus reidi	1	103·5	24·0	2·4	Serial sectioning, 3D reconstruction
Hippocampus reidi	1	119·0	25·2	2·3	CT scanning
Hippocampus zosterae	1	32·8	5·3	2·9	Clearing and staining
Hippocampus zosterae	1	29·0	5·3	2·9	CT scanning, serial sectioning
Hippocampus abdominalis	1	222·7	30·9	2·6	CT scanning, dissecting
Dunckerocampus dactyliophorus	1	103·5	25·4	1·5	CT scanning, dissecting
Dunckerocampus dactyliophorus	1	105·1	25·0	1·5	Clearing and staining
Dunckerocampus dactyliophorus	1	91·2	23·6	1·5	Serial sectioning, 3D reconstruction
Doryrhamphus melanopleura	1	41·6	11·6	2·5	Clearing and staining
Doryrhamphus melanopleura	1	56·5	13·2	2·3	CT scanning, dissecting
Doryrhamphus janssi	1	105·6	24·5	1·9	Dissecting
Doryrhamphus janssi	1	102·7	22·6	1·9	Serial sectioning
Doryrhamphus janssi	2	81·5–90·8	16·4–19·5	1·8	Clearing and staining
Corythoichthys intestinalis	2	120·8–136·2	16·4–18·2	2·2	Dissecting
Corythoichthys intestinalis	2	102·7–117·6	16·4–16·9	2·2	Clearing and staining
Corythoichthys intestinalis	1	120·2	16·1	2·3	CT scanning
Dunckerocampus pessuliferus	1	112·3	30·1	1·6	Dissecting
Dunckerocampus pessuliferus	1	94·5	26·0	1·6	Serial sectioning

CT, computed tomography.

big-belly seahorse *Hippocampus abdominalis* Lesson 1827 specimen, one *D. melanopleura* specimen, two specimens of scribbled pipefish *Corythoichthys intestinalis* (Ramsay 1881), one Janss' pipefish *Doryrhamphus janssi* (Herald & Randall 1972) specimen and one yellow banded pipefish *Dunckerocampus pessuliferus* Fowler 1938 specimen (Table I). Visualization of muscle fibre orientation was enhanced using an iodine solution (Bock & Shear, 1972).

IN TOTO CLEARING AND STAINING

Three specimens of *H. reidi*, one of *D. dactyliophorus*, two of *C. intestinalis*, one of dwarf seahorse *Hippocampus zosterae* Jordan & Gilbert 1882, one of *D. melanopleura* and two of *D. janssi* were cleared and stained for bone and cartilage according to the protocol of Taylor & Van Dyke (1985) (Table I). Specimens were dehydrated through a series of alcohol solutions prior to cartilage staining with alcian blue. Neutralization was done with saturated borax solution, followed by bleaching with 10% solution of H_2O_2 in 0·5% KOH solution and clearing in trypsin enzyme buffer solution (0·45 g in 400 ml of 30% saturated borax solution). Alizarin red S solution was used for bone staining and specimens were finally preserved in 100% glycerine.

SERIAL SECTIONS

Serial histological cross-sections of the head of a *H. reidi*, a *D. dactyliophorus*, an *H. zosterae*, a *D. pessuliferus* and a *D. janssi* specimen were made (Table I). Before sectioning, specimens stored in ethanol 70% were decalcified with Decalc 25% (Histolab Products AB; www.histolab.se), dehydrated through an alcohol series and embedded in Technovit 7100 (Heraeus Kulzer GmbH; www.heraeus-kulzer.com). Next, semi-thin sections (5 μm) were cut using a Leica Polycut SM 2500 sliding microtome (www.leica-microsystems.com) equipped with a Wolfram carbide-coated knife. Finally, sections were stained with toluidine blue, mounted on slides with xylene-based mounting medium and covered.

COMPUTED TOMOGRAPHY SCANNING

Another specimen of *H. reidi*, the dissected *D. dactyliophorus* specimen, the dissected *H. abdominalis* specimen, a specimen of *C. intestinalis*, the dissected *D. melanopleura* and the sectioned *H. zosterae* specimen were scanned at the modular micro-computed tomography (CT) set-up of Ghent University, Belgium (Masschaele *et al*., 2007) (Table I). Apart from the *H. reidi* specimen, all specimens were scanned using the transmission tube head, at 100 kV tube voltage (the *H. reidi* specimen was scanned with the directional tube head at 80 kV tube voltage). For each individual, 1200 projections of 1496 × 1880 pixels were recorded (1000 projections of 748 × 940 pixels for *H. reidi*), with an exposure time between 1·0 and 1·6 s per projection and covering 360°. The raw data were processed and reconstructed using the in-house developed CT-software Octopus (Vlassenbroeck *et al*., 2007) and rendered with myVGL 2.0.4 (Volume Graphics GmbH; www.volumegraphics.com).

GRAPHICAL 3D RECONSTRUCTIONS

Computer-generated 3D reconstructions were made to visualize musculoskeletal topography of the cranium (Figs 1, 2 and 4). Images of the histological sections were captured using a digital camera (Colorview 8, Soft Imaging System; www.microscopy.olympus.eu), mounted on a Reichert-Jung Polyvar light microscope (www.reichertms.com) and controlled by the software programme analySIS 5.0 (Soft Imaging System; www.soft-imaging.net). The digital images were imported in the software package Amira 5.1.0 (Template Graphics Software; www.amira.com). Alignment of the histological sections and tracing of the elements was done manually by superimposition to get maximal overlap of all structures. The 3D reconstruction of *H. reidi* shows a slight distortion at the level of the snout, which is probably an artefact due to the alignment (Fig. 1). This does not, however, impair the qualitative interpretations in this study.

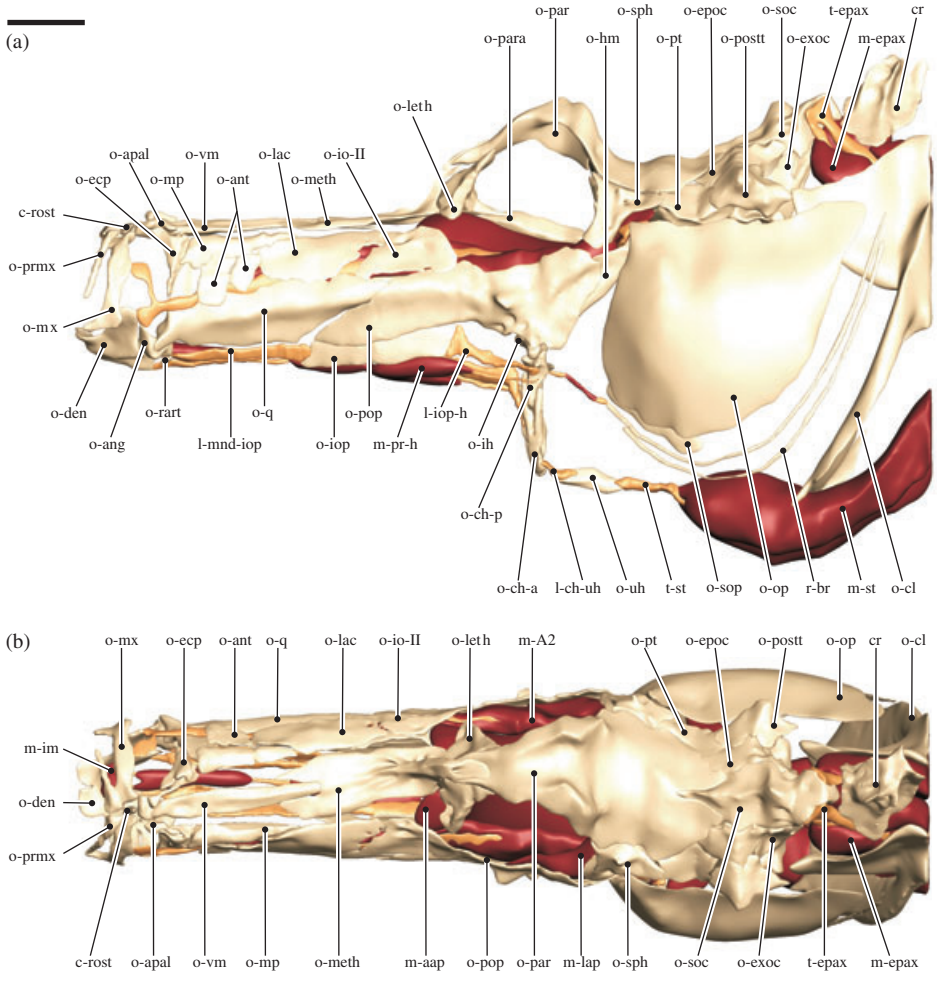

FIG. 1. 3D reconstruction of the cranium of *Hippocampus reidi* (Table I): (a) lateral view of the left side, (b) dorsal view and (c) ventral view (, bone; , cartilage; , tendon and ligament; , muscle, cr, corona; c-rost, rostral cartilage; l-ch-uh, ceratohyal-urohyal ligament; l-iop-h, interoperculo-hyoid ligament; l-mnd-h, mandibulo-hyoid ligament; l-mnd-iop, mandibulo-interopercular ligament; m-A2, second bundle of the adductor mandibulae muscle complex; m-aap, adductor arcus palatini muscle; m-epax, epaxial muscle; m-h-abd, abductor hyohyoideus muscle; m-im, intermandibularis muscle; m-lap, levator arcus palatini muscle; m-pr-h, protractor hyoidei muscle; m-st, sternohyoideus muscle; o-ang, anguloarticular bone; o-ant, antorbital bone; o-apal, autopalatine bone; o-ch-a, anterior ceratohyal bone; o-ch-p, posterior ceratohyal bone; o-cl, cleithrum; o-den, dentary bone; o-ecp, ectopterygoid bone; o-epoc, epioccipital bone; o-exoc, exoccipital bone; o-hm, hyomandibular bone; o-ih, interhyal bone; o-io-II, second infraorbital bone; o-iop, interopercular bone; o-lac, lacrimal bone; o-leth, lateral ethmoid bone; o-meth, mesethmoid bone; o-mp, metapterygoid bone; o-mx, maxillary bone; o-op, opercular bone; o-par, parietal bone; o-para, parasphenoid bone; o-pop, preopercular bone; o-postt, posttemporal bone; o-prmx, premaxillary bone; o-pt, pterotic bone; o-q, quadrate bone; o-rart, retroarticular bone; o-soc, supraoccipital bone; o-sop, subopercular bone; o-sph, sphenotic bone; o-uh, urohyal bone; o-vm, vomeral bone; r-br, branchiostegal ray; t-epax, epaxial tendon; t-pr-h, protractor hyoidei tendon; t-st, sternohyoideus tendon. Scale bar 2 mm.

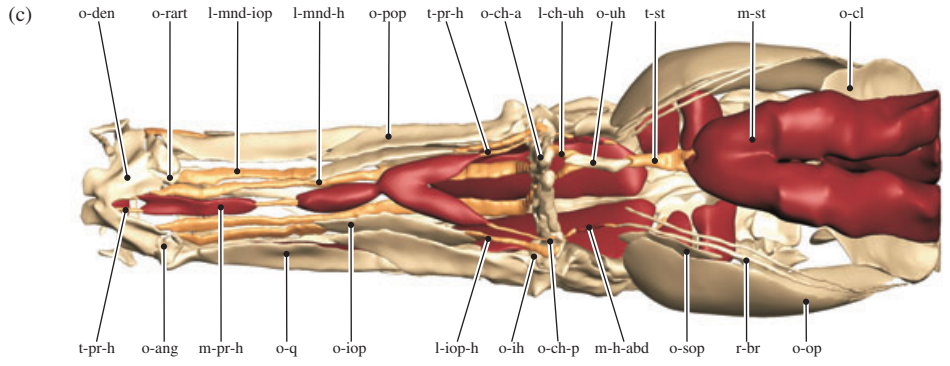

FIG. 1. Continued

TERMINOLOGY

Terminology of bony and cartilaginous elements is mostly based on Lekander (1949) and Harrington (1955). Exceptions are the vomeral, circumorbital, parietal and postparietal bones, for which the terminology of Schultze (2008) is followed. Terminology of muscles is based on Winterbottom (1974).

RESULTS

The head morphology of *H. reidi* and *D. dactyliophorus*, as representatives for the pipefish and seahorse feeding apparatus, is described. Special attention is paid to the structures related to differences in snout length.

MORPHOLOGICAL DESCRIPTION OF *H. REIDI*

Both lower jaw halves of *H. reidi* consist of Meckel's cartilage, and the dentary, the anguloarticular and the retroarticular bones. The dentary bone [Figs 1(a) and 2] bears a prominent coronoid process that is connected to the ventrolateral surface of the maxillary bone by means of the primordial ligament. Two of the adductor mandibulae muscle bundles, A1 and A2, attach onto the coronoid process [all adductor mandibulae tendons were reconstructed together (t-A) and the different attachment sites were observed on dissections; Figs 1(a) and 2]. A1 attaches by means of a slender bifurcated tendon, of which the dorsal part attaches onto the dorsomedial surface of the maxillary bone and the ventral part on the coronoid process of the dentary bone. The A1 muscle bundle [Fig. 2(a)] is situated in between the medial A3 and the lateral A2 and runs dorsally of the latter. The A2 [Figs 1(b) and 2(a)] bundle is the most lateral one, with the longest tendon and the largest muscle mass. The A3 tendon attaches ventrally on the medial face of the dentary. The short and thin A3 muscle sheet is the most medial bundle of the muscle complex. The muscle bundle is in all three cases much longer than the tendon in front of the muscle and they all run almost in a straight line. The dentary bone is provided with a tube-like cavity in which the tapering end of the anguloarticular bone fits. At the medial side of the dentary bone, the stout mandibulo-hyoid ligament [Figs 1(c) and 2] attaches ventrocaudally, which is connected to the anterior ceratohyal bone. More rostrally and

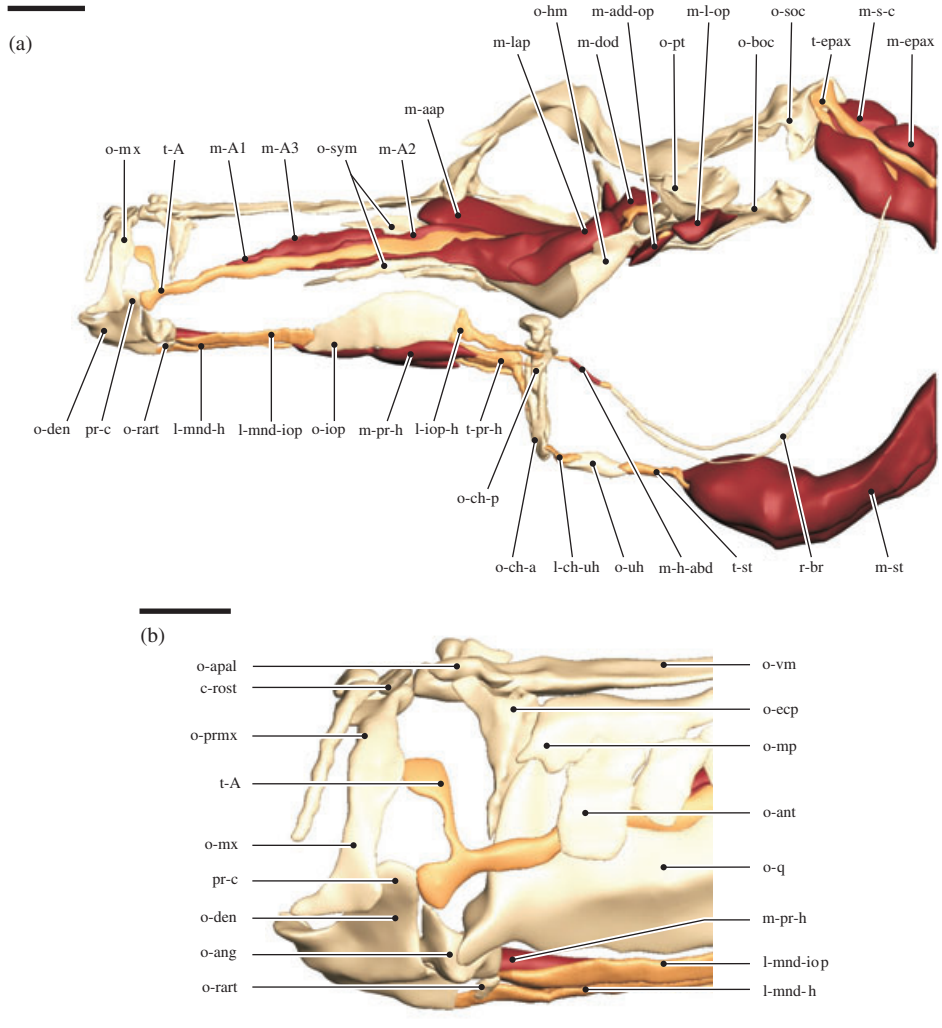

FIG. 2. 3D reconstruction of the cranium of *Hippocampus reidi* (Table I): (a) lateral view of the left side with several bones removed to show muscles underneath and (b) lateral view of the left side of the snout tip (, bone; , cartilage; , tendon and ligament; , muscle). c-rost, rostral cartilage; l-ch-uh, ceratohyal-urohyal ligament; l-iop-h, interoperculo-hyoid ligament; l-mnd-h, mandibulo-hyoid ligament; l-mnd-iop, mandibulo-interopercular ligament; m-A1, first bundle of the adductor mandibulae muscle complex; m-A2, second bundle of the adductor mandibulae muscle complex; m-A3, third bundle of the adductor mandibulae muscle complex; m-aap, adductor arcus palatini muscle; m-add-op, adductor operculi muscle; m-dod, dilatator operculi dorsalis muscle; m-epax, epaxial muscle; m-h-abd, abductor hyohyoideus muscle; m-lap, levator arcus palatini muscle; m-l-op, levator operculi muscle; m-pr-h, protractor hyoidei muscle; m-s-c, supracarinalis muscle; m-st, sternohyoideus muscle; o-ang, anguloarticular bone; o-ant, antorbital bone; o-apal, autopalatine bone; o-boc, basioccipital bone; o-ch-a, anterior ceratohyal bone; o-ch-p, posterior ceratohyal bone; o-den, dentary bone; o-ecp, ectopterygoid bone; o-hm, hyomandibular bone; o-iop, interopercular bone; o-mp, metapterygoid bone; o-mx, maxillary bone; o-prmx, premaxillary bone; o-pt, pterotic bone; o-q, quadrate bone; o-rart, retroarticular bone; o-soc, supraoccipital bone; o-sym, symplectic bone; o-uh, urohyal bone; o-vm, vomeral bone; pr-c, coronoid process; r-br, branchiostegal ray; t-A, adductor mandibulae muscle complex tendon; t-epax, epaxial tendon; t-pr-h, protractor hyoidei tendon; t-st, sternohyoideus tendon. Scale bar (a) 2 mm and (b) 1 mm.

close to the dentary symphysis, there is a small attachment site of the thin protractor hyoidei tendon [Fig. 1(c)]. The protractor hyoidei muscle [Figs 1(a), (c), 2(a) and 3(a)] runs ventrally to the mandibulo-hyoid ligament and attaches to the posterior ceratohyal bone (Roos *et al.,* 2009*a*, provides a detailed description of this muscle). The intermandibularis muscle [Fig. 1(c)] connects left and right dentary bones. The dentary bone and anguloarticular bone [Figs 1(a) and 2] are firmly fixed to each other by connective tissue and form a single functional unit. Caudally, the anguloarticular bone forms a saddle-shaped cartilaginous articulation for the quadrate bone. The retroarticular bone [Figs 1(a), (c) and 2] is a very small bone that is connected to the interopercular bone by means of a firm mandibulo-interopercular ligament.

Both the premaxillary and maxillary bones are reduced and toothless bones, which articulate with each other dorsally. A short ligamentous sheet connects the premaxillary bone [Figs 1(a), (b) and 2] to the maxillary bones rostrally. The maxillary bone [Figs 1(a), (b) and 2] has a broadening ventral part where the primordial ligament attaches. In between the left and right maxillary bones, a rostral cartilage is situated, which is enclosed by a large ligament that runs to the vomeral bone. The maxillary bones articulate with the cartilage dorsally to the vomeral bone.

The suspensorium forms the lateral wall of the tubular snout and most elements are therefore elongated. The small autopalatine bone [Figs 1(a), (b) and 2(b)] articulates cartilaginously with the ethmoid cartilage dorsal to the vomeral bone. This forms the rostral one of the two articulations that movably connect the suspensorium to the neurocranium. The tendons of the adductor mandibulae muscle complex [Fig. 3(b)] run laterally to the quadrate and medially to the circumorbital bones. The A1 and A3 bundles of the complex [Fig. 2(a)] attach on the caudal and rostral part of this dorsal crest of the symplectic bone, respectively. Bundle A2 of the adductor mandibulae muscle complex attaches on the medial face of the preopercular and hyomandibular bones. The hyomandibular bone [Fig. 2(a)] bears a dorsorostrally and a dorsocaudally oriented articulation head that fit respectively into a socket on the ventral surface of the sphenotic bone and in the cartilaginous surface between the sphenotic, the prootic and the pterotic bones.

The interhyal bone [Figs 1(a), (c) and 2(a)] provides the articulation between the suspensorium and the other elements of the hyoid, which form a rigid unit. It bears two heads in between which the posterior ceratohyal bone [Figs 1(a), (c) and 2(a)] articulates. The bone tapers ventrally where there is a firm synchondrosis with the anterior ceratohyal bone. The anterior ceratohyal bone [Figs 1(a), (c) and 2(a)] has a somewhat triangular shape with a small but firm symphysis between the left and right bones close to their distal apices. The urohyal bone [Figs 1(a), (c) and 2(a)] is a small, blunt bone, measuring less than the total hyoid length. The short tendon of the sternohyoideus muscle [Figs 1(a), (c) and 2(a)] encloses the urohyal bone almost entirely at its caudal tip. It is a very large muscle, which incorporates its tendon entirely [Fig. 3(c)]. More details about the hyoid of *H. reidi* can be found in Roos *et al*. (2009*a*).

The supraoccipital bone [Figs 1(a), (b) and 2(a)] tapers caudally where it touches the corona (*i.e.* the first postcranial bony plate). At the centre of the supraoccipital caudal surface, the supracarinalis muscle attaches, which runs to the neural arch of the first vertebra and to the second postcranial bony plate [Figs 2(a) and 3(d)]. Laterally to the supracarinalis muscle attachment, the well-developed epaxial muscle attaches by means of two large, but short tendons [Fig. 3(d)]. The exoccipital bone

[Fig. 1(a), (b)] is ligamentously connected to the dorsorostral tip of the cleithrum. The basioccipital bone [Fig. 2(a)] bears the occipital joint and it interdigitates ventrally with the parasphenoid bone. The occipital joint has a ventrocaudal orientation, contributing to the angle between the head and the body in *H. reidi*.

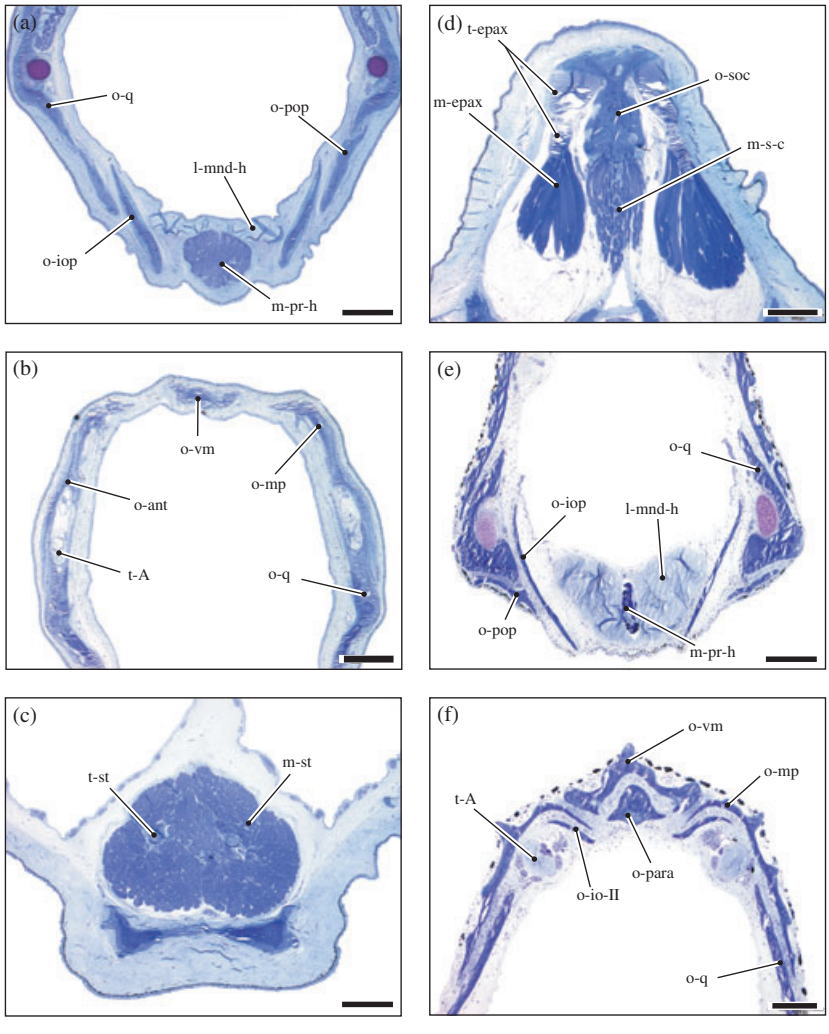

FIG. 3. Histological cross-sections of the cranium of (a)–(d) *Hippocampus reidi* (Table I) and (e)–(h) *Dunckerocampus dactyliophorus* (Table I) stained with toluidine blue. (a), (e) The nasal region showing the mandibulo-hyoid ligament and the protractor hyoidei muscle organisation. (b), (f) The sternohyoideus muscle and its tendon. (c), (g) The snout rostrally with the adductor mandibulae tendon. (d), (h) The occipital region with the supraoccipital bone and its associated tendons and muscles, note the sesamoid bone in *D. dactyliophorus*. l-mnd-h, mandibulo-hyoid ligament; m-epax, epaxial muscle; m-pr-h, protractor hyoidei muscle; m-s-c, supracarinalis muscle; m-st, sternohyoideus muscle; o-ant, antorbital bone; o-epax, sesamoid bone in epaxial tendon; o-io-II, second infraorbital bone; o-iop, interopercular bone; o-mp, metapterygoid bone; o-pop, preopercular bone; o-para, parasphenoid bone; o-q, quadrate bone; o-soc, supraoccipital bone; o-vm, vomeral bone; t-A, adductor mandibulae muscle complex tendon; t-epax, epaxial tendon; t-st, sternohyoideus tendon. Scale bars (a)–(d) 500 μm and (e)–(h) 200 μm.

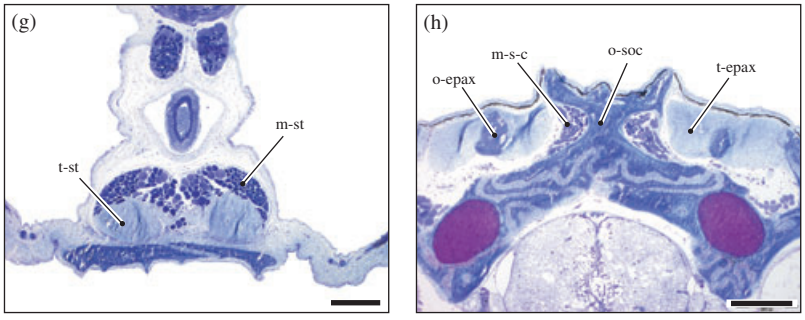

FIG. 3. Continued

MORPHOLOGICAL DESCRIPTION OF *D. DACTYLIOPHORUS*

The description of the cranium of *D. dactyliophorus* will be limited to those features in which it differs from *H. reidi*. The dentary bone [Figs 4(a), (c) and 5] is provided with a prominent lateral crest and the coronoid process is less developed. The adductor mandibulae muscle complex [Figs 4(a) and 5] consists of only two muscle bundles; a ventral one (thought to be homologous to the A2) and a dorsal one (probably homologous to A3) that attach both with a very long tendon onto the coronoid process of the dentary bone. The fusion with the anguloarticular bone [Figs 4(a), (c) and 5(b)] seems to be more firm compared to *H. reidi*, as well as it has a larger process forming the posterior part of the coronoid process. The tendon of the protractor hyoidei muscle [Figs 4(c) and 5(a)] attaches further away from the symphysis between the left and right dentary bone. The muscle is interrupted by a dense connective tissue three times. Strikingly, the fibres of the protractor hyoidei muscle are enclosed by the heavily built mandibulo-hyoid ligament [Figs 3(e) and 4(c)], leaving only the rostral and caudal bifurcating ends free.

The rostral suspensorio-neurocranial articulation is a hinge joint consisting of two small projections of the autopalatine bone [Figs 4(a), (b) and 5(b)] with a cartilaginous part of the vomeral bone in between. The muscles of the adductor mandibulae complex [Fig. 3(f)] run dorsally in the snout, rostrally supported by a ridge of the quadrate bone. The A2 muscle attaches on the medial surface of the preopercular bone (Fig. 4) and caudally on the dorsal crest of the symplectic bone [Figs 4(a) and 5(a)]. Bundle A3 of the adductor mandibulae muscle attaches rostrally on the dorsal crest as in *H. reidi* [Fig. 5(a)]. The interoperculo-hyoid ligament and the tendon of the protractor hyoidei muscle attach, respectively, rostrally and just ventrally to a lateral, knob-like process of the posterior ceratohyal bone [Figs 4(a), (c) and 5(a)]. The apices of the left and right anterior ceratohyal bone [Fig. 4(a), (c)] do not diverge very much and the symphysis is located more distal compared to *H. reidi*. The urohyal bone [Figs 4(a), (c) and 5(a)] is long, more than three times the hyoid length. The sternohyoideus muscle [Figs 4(a), (c) and 5(a)] is not as large as that in *H. reidi*, and the well-developed tendon is not incorporated by the muscle [Fig. 3(g)].

The supraoccipital bone [Figs 3(h), 4(a), (b) and 5(a)] has a biconcave profile in cross-section where it is provided with clear attachment sites for the postcranial muscles. Together with the epioccipital bone [Fig. 4(a), (b)], the supraoccipital bone encloses a cavity for the very solid tendon of the slender epaxial muscle. Interestingly,

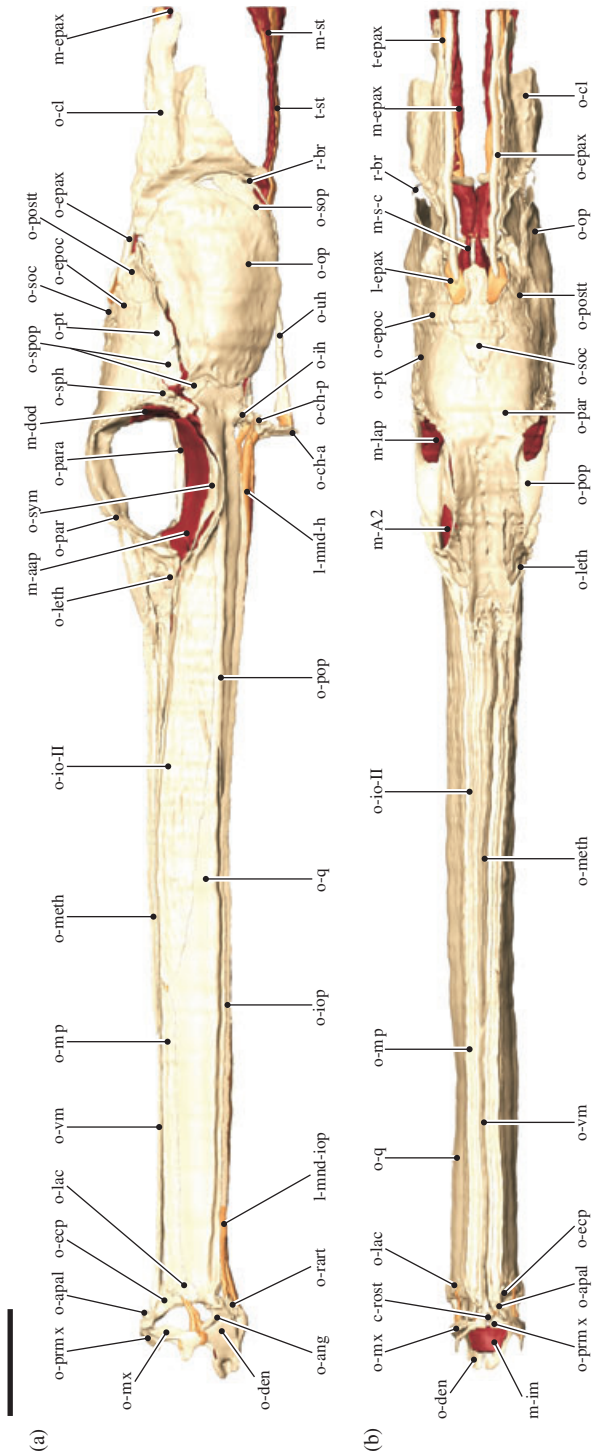

FIG. 4. 3D reconstruction of the cranium of *Danckerocampus dactyliophorus* (Table I): (a) lateral view of the left side; (b) dorsal view and (c) ventral view (■, bone; ■, cartilage; ■, tendon and ligament; ■, muscle). c-rost, rostral cartilage; l-epax, epaxial ligament; l-iop-h, interoperculo-hyoid ligament; l-mnd-h, mandibulo-hyoid ligament; l-mnd-iop, mandibulo-interopercular ligament; l-prim, primordial ligament; m-A2, second bundle of the adductor mandibulae muscle complex; m-aap, adductor arcus palatini muscle; m-dod, dilatator operculi dorsalis muscle; m-epax, epaxial muscle; m-h-abd, abductor hyohyoideus muscle; m-im, intermandibularis muscle; m-lap, levator arcus palatini muscle; m-pr-h, protractor hyoidei muscle; m-s-c, supracarinalis muscle; m-st, sternohyoideus muscle; o-ang, anguloarticular bone; o-apal, autopalatine bone; o-bh, basihyal bone; o-ch-a, anterior ceratohyal bone; o-ch-p, posterior ceratohyal bone; o-cl, cleithrum; o-den, dentary bone; o-ecp, ectopterygoid bone; o-epax, sesamoid bone in epaxial tendon; o-epoc, epioccipital bone; o-ih, interhyal bone; o-io-II, second infraorbital bone; o-iop, interopercular bone; o-lac, lacrimal bone; o-leth, lateral ethmoid bone; o-meth, mesethmoid bone; o-mp, metapterygoid bone; o-mx, maxillary bone; o-op, opercular bone; o-par, parietal bone; o-para, parasphenoid bone; o-pop, preopercular bone; o-postt, posttemporal bone; o-prmx, premaxillary bone; o-pt, pterotic bone; o-q, quadrate bone; o-rart, retroarticular bone; o-soc, supraoccipital bone; o-sop, suboperculare bone; o-sph, sphenotic bone; o-spop, supraopercular bone; o-sym, symplectic bone; o-uh, urohyal bone; o-vm, vomeral bone; r-br, branchiostegal ray; t-epax, epaxial tendon; t-h-abd; hyohyoideus abductor tendon; t-pr-h, protractor hyoidei tendon; t-st, sternohyoideus tendon. Scale bar 2 mm.

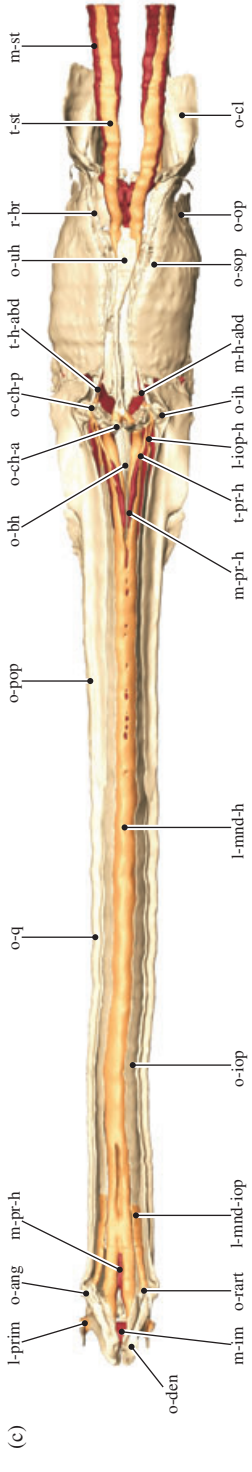

FIG. 4. Continued

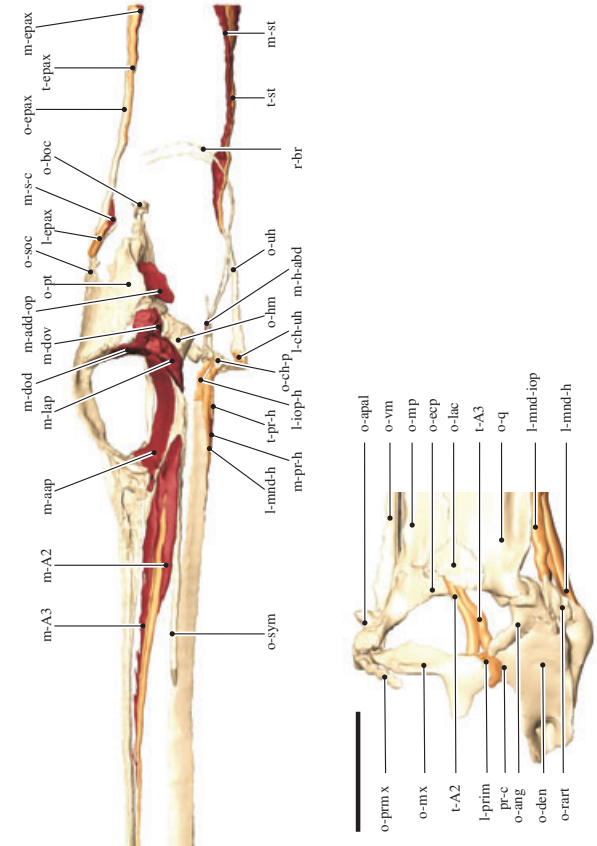

FIG. 5. 3D reconstruction of the cranium of *Dunckerocampus dactyliophorus* (Table I): (a) lateral view of the left side with several bones removed to show muscles underneath and (b) lateral view of the left side of the snout tip (, bone; , cartilage; , tendon and ligament; , muscle). l-ch-uh, ceratohyal-urohyal ligament; l-epax, epaxial ligament; l-iop-h, interoperculo-hyoid ligament; l-mnd-h, mandibulo-hyoid ligament; l-mnd-iop, mandibulo-interopercular ligament; l-prim, primordial ligament; m-A2, second bundle of the adductor mandibulae muscle complex; m-A3, third bundle of the adductor mandibulae muscle complex; m-aap, adductor arcus palatini muscle; m-add-op, adductor operculi muscle; m-dod, dilatator operculi dorsalis muscle; m-dov, dilatator operculi ventralis muscle; m-epax, epaxial muscle; m-h-abd, abductor hyohyoideus muscle; m-lap, levator arcus palatini muscle; m-pr-h, protractor hyoidei muscle; m-s-c, supracarinalis muscle; m-st, sternohyoideus muscle; o-ang, anguloarticular bone; o-apal, autopalatine bone; o-boc, basioccipital bone; o-ch-p, posterior ceratohyal bone; o-den, dentary bone; o-ecp, ectopterygoid bone; o-epax, sesamoid bone in epaxial tendon; o-hm, hyomandibular bone; o-iop, interopercular bone; o-lac, lacrimal bone; o-mp, metapterygoid bone; o-mx, maxillary bone; o-prmx, premaxillary bone; o-pt, pterotic bone; o-q, quadrate bone; o-rart, retroarticular bone; o-soc, supraoccipital bone; o-sym, symplectic bone; o-uh, urohyal bone; o-vm, vomeral bone; pr-c, coronoid process; r-br, branchiostegal ray; t-A2, second tendon of the adductor mandibulae muscle complex; t-A3, third tendon of the adductor mandibulae muscle complex; t-epax, epaxial tendon; t-pr-h, protractor hyoidei tendon; t-st, sternohyoideus tendon. Scale bar (a) 2 mm and (b) 1 mm.

within the tendon, a very long bony rod is embedded. The rostral part of the tendinous tissue is in fact a short, but firm ligament that connects the supraoccipital bone to this sesamoid bone. The occipital joint, formed by the basioccipital bone [Fig. 5(a)], is oriented caudally so that the cranium and vertebral column lie on the same axis.

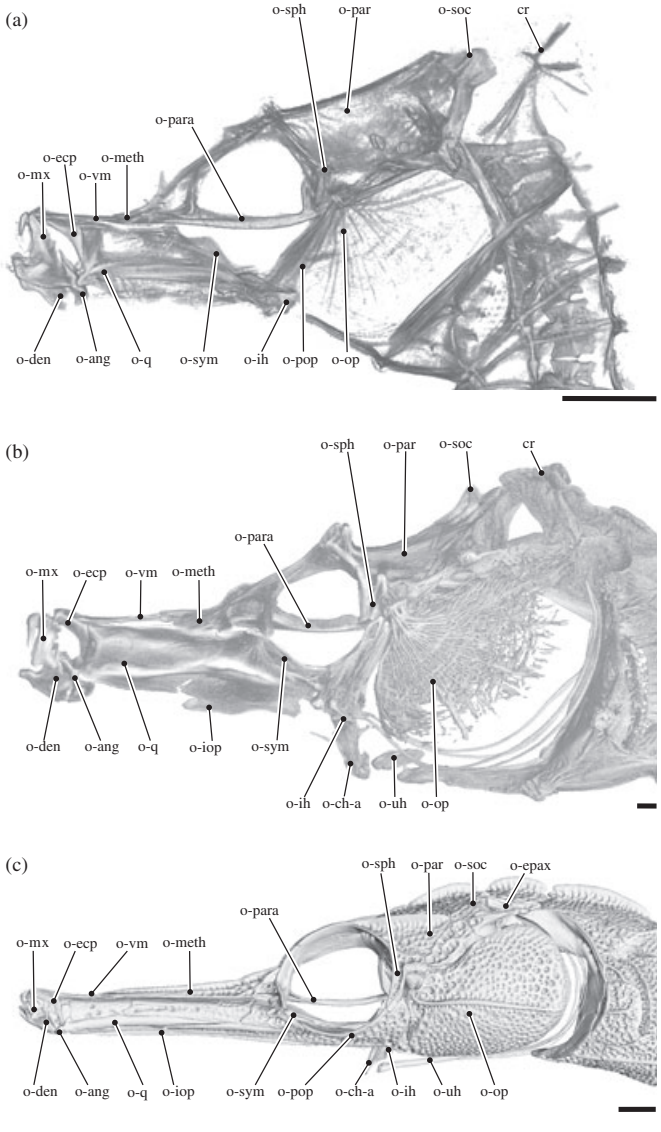

FIG. 6. 3D reconstructions of the osteocranium in lateral view of (a) *Hippocampus zosterae*, (b) *Hippocampus abdominalis*, (c) *Corythoichthys intestinalis* and (d) *Doryrhamphus melanopleura* (Table I). cr, corona; o-ang, anguloarticular bone; o-ch-a, anterior ceratohyal bone; o-den, dentary bone; o-ecp, ectopterygoid bone; o-epax, sesamoid bone in epaxial tendon; o-ih, interhyal bone; o-iop, interopercular bone; o-meth, mesethmoid bone; o-mx, maxillary bone; o-op, opercular bone; o-par, parietal bone; o-para, parasphenoid bone; o-pop, preopercular bone; o-q, quadrate bone; o-soc, supraoccipital bone; o-sph, sphenotic bone; o-sym, symplectic bone; o-uh, urohyal bone; o-vm, vomeral bone. Scale bars 1 mm.

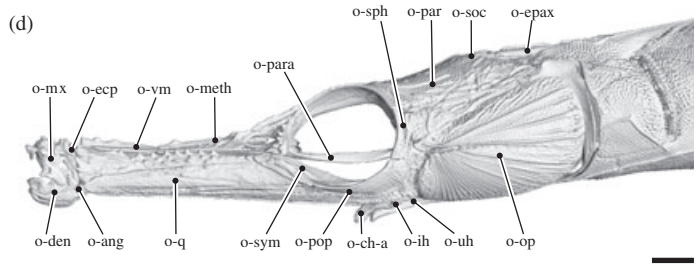

FIG. 6. Continued

OTHER SYNGNATHID SPECIES

For the comparison with the other pipefish and seahorse species, only those features that might be related to snout elongation are treated. *Hippocampus zosterae* [Fig. 6(a)] is a small short-snouted seahorse. The articulation between autopalatine and vomeral bone involves less cartilage than the one in *H. reidi*. The dentary and anguloarticular bones interdigitate rather loosely and the coronoid process is low with respect to the length of the lower jaw long axis. The adductor mandibulae tendons are much shorter than the muscle bundles and the protractor hyoidei muscle, which is not enclosed by the mandibulo-hyoid ligament, attaches mediorostrally on the dentary. The hyoid is a very solid structure with a firm ceratohyal symphysis. As is the case in *H. reidi*, the urohyal length is less than the hyoid length and the sternohyoideus muscle is of substantial size. There is no sesamoid bone in the short epaxial tendon and the epaxial muscle is well developed.

In *H. abdominalis* [Fig. 6(b)], a larger seahorse with intermediate snout length, the angular and dentary bones are not very firmly interdigitated and the dentary bone is provided with a high coronoid process. The adductor mandibulae muscle complex runs approximately in a horizontal line caudally and only about a fourth of its length consists of just tendon. The anterior part of the vomeral bone broadens somewhat and at its rostral end it articulates with the autopalatine bone by means of a point articulation. Like *H. reidi* and *H. zosterae*, the urohyal bone of *H. abdominalis* is shorter than the hyoid and no epaxial sesamoid bone is present. The protractor hyoidei muscle, however, is enclosed by the firm mandibulo-hyoid ligament for almost its entire length, similar to the situation in *D. dactyliophorus*. The protractor hyoidei tendon attaches on the ventromedial surface of the dentary bone, rostral to the mandibulo-hyoid ligament attachment site. Somewhat more caudally, the ligament incorporates the muscle and only the caudal third of the protractor hyoidei muscle is left free. Here, the left and right bundles diverge and run ventrally of the ligament to respectively the posterior and anterior ceratohyal bone, where they attach. The sternohyoideus and epaxial muscles are both well developed and have short tendons.

Corythoichthys intestinalis [Fig. 6(c)] has a short but very slender snout. Its skull bones are covered with many small indentations, especially at the level of the braincase, the opercular bone and caudally on the preopercular bone. The vomeral bone is very slim and provides a simple articulation with the autopalatine bone rostrally. Also the dentary bone is slender and its rostral part is bent upwards to almost the same height as the well-developed coronoid process. The anguloarticular bone is fairly well attached to the dentary bone. The protractor hyoidei muscle and mandibulo-hyoid

ligament run separately to the posterior and anterior ceratohyal bones, respectively. The length of the adductor mandibulae tendons is small in comparison to the muscle length. The symphysis between left and right anterior ceratohyal bones is large, taking up almost half of the total hyoid length. The urohyal bone is long, being more than two times the hyoid length, and has a small bifurcation caudally. The sternohyoideus and epaxial muscles are smaller than the ones in *H. reidi*, but their tendons are not as long as in *D. dactyliophorus*. Nevertheless, *C. intestinalis* has a long and slender ossified rod within the tendon of the epaxial muscle. The ligamentous part that connects the supraoccipital bone with this rod, however, is shorter than in *D. dactyliophorus*. Like all pipefishes, *C. intestinalis* has a caudally oriented occipital joint, with no angle between the head and the body.

In *D. melanopleura* [Fig. 6(d)], also a short-snouted pipefish, the snout and maxillary bones are covered with small protuberances. The occipital joint, which has a caudal orientation, is elliptically shaped and quite broad. The lower jaw in *D. melanopleura* has a fairly solid connection between the separate elements and a relatively high coronoid process. The protractor hyoidei muscle is not enclosed by the mandibulo-hyoid ligament in *D. melanopleura.* The tendons of the sternohyoideus and the epaxial muscle are all relatively long. The two muscles also have a smaller diameter than the muscles of the studied *Hippocampus* sp. Honshu pipefish *Doryrhamphus melanopleura*, like *D. dactyliophorus* and *C. intestinalis*, which has a long and slender sesamoid bone within the tendon of the epaxial muscle. The urohyal bone is long, exceeding the hyoid three times in length, and the caudal bifurcation is large, almost reaching the cleithrum.

The cranium of the long-snouted *D. pessuliferus* and *D. janssi* is quite similar to the one in *D. dactyliophorus*. The lower jaw of *D. janssi* looks like the one in *D. dactyliophorus*, with a low coronoid process and robust connection between dentary and anguloarticular bone. The mandibulo-hyoid ligament, however, does not enclose the protractor hyoidei muscle. In *D. pessuliferus*, the lower jaw interdigitation is also firm and in addition, the protractor hyoidei muscle is enclosed by the mandibulo-hyoid ligament. In both species, the part of the adductor mandibulae complex that consists solely of tendon is approximately half the total length and the muscle runs dorsally in the snout. The hinge joint between the autopalatine and the vomeral bone found in *D. dactyliophorus* is a simple point-joint in these two species here. All three species have a very long urohyal bone, but in both *D. pessuliferus* and *D. janssi*, it is a forked, very slender rod. In the latter, the urohyal bone keeps running in between the hypaxial muscle bundles even well beyond the pectoral fin, reaching a length of over six times the hyoid length, which is almost as long as the entire snout. In *D. pessuliferus*, the urohyal length is only somewhat more than two times the hyoid length. Their sternohyoideus muscle, which is not very large, has a well-developed tendon, similar to the situation found in *D. dactyliophorus*. Both *D. pessuliferus* and *D. janssi* are in the possession of a long and slim sesamoid bone in the long epaxial tendon.

DISCUSSION

Pipefishes and seahorses are pivot feeders; they capture mobile prey by means of a rapid dorsorotation of the head in combination with an equally fast expansion

of the buccal cavity. Syngnathid pivot feeding starts with hyoid rotation, which is followed by neurocranial elevation (both movements are coupled in a four-bar mechanism; Muller, 1987; Van Wassenbergh *et al*., 2008; Roos *et al*., 2009*a*). Next, the mouth is opened, the snout is expanded and the prey is sucked in after only *c*. 6 ms (Bergert & Wainwright, 1997; de Lussanet & Muller, 2007; Roos *et al*., 2009*b*). The specialized feeding strategy is hypothesized to be associated with morphological modifications and innovations of the feeding apparatus, especially with respect to the snout. Therefore, the morphology of the main cranial elements will be discussed in a functional context first. In the next part of the discussion, the structural variation in the cranium of all syngnathids studied here is considered in an attempt to assess the implication of variation in snout length on the head morphology.

SPECIALIZED FEEDING STRATEGY

The syngnathid species studied all have a fused dentary and anguloarticular bone, as well as a saddle-shaped quadrato-mandibular joint and a firm but mobile dentary symphysis. The hyoid configuration resembles the one of the lower jaw in having a solid synchondrosis between the anterior and posterior ceratohyal bones, a saddle-shaped interhyo-ceratohyal articulation and a strong and flexible ceratohyal symphysis. Besides the special lower jaw and hyoid morphology, the maxillary bones are much reduced in size and the pectoral girdle is immovably connected to the vertebrae. Although these traits are not necessarily syngnathid synapomorphic characters, they might be related to the pivot feeding. These features and their assumed role during suction feeding are elaborated on, based on the morphology of *H. reidi* and *D. dactyliophorus*.

All three elements of each lower jaw half (dentary, anguloarticular and retroarticular bones) function as a single unit that articulates by means of a saddle joint with the suspensorium. This type of articulation permits only rotation in a sagittal plane, resulting in mouth opening and closing. Theoretically, lower jaw depression can be accomplished in three different ways: the mandibulo-hyoid ligament translates hyoid rotation into mouth opening, the mandibulo-interopercular and interopercular-hyoid ligaments form a second coupling between the hyoid rotation and the lower jaw depression, and contraction of the protractor hyoidei muscle will also open the mouth [note that an opercular four-bar mechanism for depressing the lower jaw (Anker, 1974; Westneat, 1990; Hunt von Herbing *et al*., 1996; Van Wassenbergh *et al*., 2005) is not functional in syngnathids as there is no connection between the opercular and interopercular bones]. When the mouth of *H. reidi* is closed, the line of action of the protractor hyoidei muscle lies dorsal to the quadrato-mandibular joint, so contraction will not result in lower jaw depression, but instead the muscle will probably be strained and elastic energy will be stored [similar to the catapult mechanism in the epaxial muscle of syngnathids (Van Wassenbergh *et al*., 2008)]. Both *H. reidi* and *D. dactyliophorus* specimens used for the 3D reconstructions have their hyoid and lower jaw depressed, but the mandibulo-hyoid ligament does not seem to be fully extended, as it is curved ventrally along the hyoid. This could suggest that the ligament contributes only to the initial phase of mouth opening, resulting in lowering of the dentary (and thus also of the protractor hyoidei tendon attachment site) until the muscle line of action shifts to below the lower jaw articulation. Further lower jaw depression could then be the consequence of a sudden release of the

strain energy stored in the protractor hyoidei muscle-tendon system. The mandible would then rotate further ventrally due to its own inertia, causing the slack status of the mandibulo-hyoid ligament. The tendinous interruptions of the protractor hyoidei muscle would be especially beneficial because tendons are better suited for storing elastic strain energy than muscle tissue is (Alexander & Bennet-Clark, 1977).

The mouth is closed again through the contraction of the adductor mandibulae complex, in combination with the rotation of the hyoid to its resting position and the relaxation of the mandibular ligaments and protractor hyoidei muscle. Lower jaw adduction is also accomplished by contraction of the intermandibularis muscle that attaches close to the dentary symphysis and perhaps indirectly by contraction of the adductor arcus palatini muscle, which will adduce the suspensoria (the latter muscle might also be responsible for the initial locking of the cranial four-bar system prior to neurocranial elevation (G. Roos, H. Leysen, S. Van Wassenbergh, P. Aerts, A. Herrel & D. Adriaens, unpubl. data).

Syngnathids do not have a typical teleostean hyoid configuration with a ball and socket joint between the interhyal and the hyomandibular bones. Instead, the interhyal bone has a rounded dorsal head that articulates with the preopercular bone and two large ventral processes that form a saddle-shaped articulation with the posterior ceratohyal bone. As in the lower jaw, this type of joint will limit the translational and rotational degrees of freedom of the articulation and may facilitate muscle action to be transferred strictly unto hyoid depression. This may reduce the risk of dislocation during fast and powerful hyoid depression, powered by the contraction of the sternohyoideus muscle. At first, all elements of the hyoid will rotate as a single rigid unit with respect to the preopercular bone. At a certain angle, however, this rotation seems to become restrained and from that point on, the interhyal bone remains immobile and the posterior ceratohyal bone starts articulating with respect to it. The angle over which the hyoid turns during suction feeding is $>90^{\circ}$. Hence, once beyond the point of 90°, there is no direct contribution of hyoid depression to buccal volume increase through a lowering of the buccal floor. Indirectly, however, hyoid depression does contribute to oral expansion *via* suspensorial abduction, which is the main cause of buccal volume increase (Roos *et al*., 2009*b*). When the hyoid is protracted, the two anterior ceratohyal bones lay at an angle with respect to each other in a way that both hyoid bars and the symphyseal hinge axis do not fall in the same plane. Contraction of the sternohyoideus muscle will therefore not only result in hyoid depression but also in rotation of the hyoid bars at their symphysis (Aerts, 1991). This rotation will move left and right hyoid outwards along their long axis; hence, the suspensoria will be abducted. This might be aided by contraction of the levator arcus palatini muscle.

In all species studied here, the maxillary bones are very much reduced and toothless. Their contribution to the buccal volume increase during suction will not be substantial given the absence of upper jaw protrusion nor are they used for grasping the prey as prey is exclusively caught by suction.

There is a small overlap between the cleithrum of the pectoral girdle on the one hand and both exoccipital and post-temporal bones on the other (a supracleithrum is absent). As the pectoral girdle is firmly attached to the vertebral column, this overlap forms two extra articulations (left and right) between the cranium and the vertebropectoral complex, besides the occipital joint. These three articulation points all lay on the same axis, so fast neurocranial elevation with a reduced risk of dislocation

is possible. Unlike the situation in syngnathids, in most actinopterygians there is no connection between the girdle and the vertebral column and most elements of the shoulder girdle articulate with each other, resulting in a very mobile structure (Gosline, 1977). In three-spined stickleback *Gasterosteus aculeatus* L. 1758, there is a supracleithrum that is movably connected to the posttemporal bone rostrally and to the cleithrum caudally (Anker, 1974). In addition, a small costa and connective tissue provides the connexion between the cleithrum and the transverse process of the first vertebra (Anker, 1974). This situation, *i.e.* the reduced mobility compared to the typical actinopterygian configuration, may be regarded as the plesiomorphic condition to the syngnathid configuration. On the supraoccipital bone, the supracarinalis muscle and the tendon of the epaxial muscle attach. The epaxial muscle and its tendon are involved in a power-amplifier system, which makes the extremely high-velocity rotation of the head in syngnathids possible (Van Wassenbergh *et al*., 2008). The supracarinalis muscle is connected to the first vertebra and might also be associated with neurocranial elevation during suction feeding.

VARIATION RELATED TO SNOUT LENGTH

The morphology of the lower jaw and hyoid is very similar in all species studied here, regardless of their snout phenotype. This conservative morphology is precisely what was expected in these high performance suction feeders, as even a tiny change in the complex integrated system could have a negative effect on the feeding performance (Adriaens & Herrel, 2009). Some variation related to differences in snout length, however, was expected, as an elongation of the snout is thought to influence the efficiency of the mechanics of the lever systems in the head.

Increase in snout length implies there has to be an elongation of either the adductor mandibulae tendon or the muscle complex. Because powerful jaw closure is not required in suction feeding, elongation of the tendon instead of the muscle is energetically more favourable. An additional advantage of tendon over muscle elongation is that tendinous tissue occupies less space. This is reflected in the jaw muscle morphology of the species with the longest snouts: in *D. dactyliophorus*, *D. pessuliferus* and *D. janssi* the tendons of the adductor mandibulae are all very long, with approximately half of the distance between origin and insertion being covered by tendon alone. Besides that, elongation of the adductor mandibulae complex is expected to be associated with changes in the coronoid height, onto which the muscle attaches, or in the muscle line of action to maintain kinematic efficiency. The angle between the axis connecting the jaw joint with the attachment site of the adductor mandibulae muscle on the coronoid process (*i.e.* the in-lever arm) and the line of action of the muscle will decrease with increasing snout length. This will reduce the mechanical advantage of the lever system. The mechanical advantage increases with the elongation of the in-lever arm; hence, a higher coronoid process is hypothesized to be present in long-snouted species. The coronoid process is low with respect to the length of the lower jaw in both short- and long-snouted species (*D. dactyliophorus*, *D. janssi*, *C. intestinalis* and *H. zosterae*), whereas others (*H. reidi*, *H. abdominalis*, *D. melanopleura* and *D. pessuliferus*) have a relatively high coronoid process. Therefore, the hypothesis does not hold true. The path of the adductor mandibulae muscle, however, is more arched in the long-snouted pipefishes (*D. pessuliferus* and *D. dactyliophorus*), and the muscle is at the snout tip ventrally supported by

a ridge of the quadrate that probably prevents it from lowering during contraction. Hence, the muscles line of action at the level of the attachment site on the dentary is orientated more dorsally. This will probably result in an increased angle with the in-lever arm and could hence increase the mechanical advantage of the lower jaw lever system.

If the protractor hyoidei muscle is strained prior to mouth opening, as suggested in the first part of the discussion and based on kinematic data (Roos *et al*., 2009*b*), torque might be induced between the separate elements of the lower jaw. This could be more of an issue in long-snouted species, as more elastic strain energy can be stored in the long protractor hyoidei muscle and its tendon. Therefore, an increase in the amount of interdigitation and ligamentous connection between the anguloarticular and dentary bones with increasing snout length was hypothesized. In seahorses, the dentary-anguloarticular interdigitation ranged from loosely (*H. zosterae*) over intermediate (*H. abdominalis*) to rather firm (*H. reidi*) with increasing snout length, supporting the hypothesis. In addition, long-snouted pipefishes (*D. dactyliophorus*, *D. pessuliferus* and *D. janssi*) seem to have a tighter connection between the elements of the lower jaw than some shorter snouted species do, like *C. intestinalis* and Nilsson's pipefish *Syngnathus rostellatus* Nilsson 1855 (Leysen *et al*., 2010). Another short-snouted pipefish, *D. melanopleura*, however, has quite a firmly interdigitated lower jaw as well.

The sternohyoideus muscle is confluent with the hypaxial muscle, which plays an important role in the coupling of hyoid rotation and neurocranial elevation (Muller, 1987; Van Wassenbergh *et al*., 2008; Roos *et al.,* 2009*a*). Before prey capture, the epaxial and hypaxial muscles contract and tension is built up in both tendons (Van Wassenbergh *et al*., 2008). This energy is suddenly released when the four-bar mechanism is unlocked, resulting in powerful movements of the hyoid and head. Snout elongation will increase the moment of inertia of the head; hence, an increased force is needed to overcome this during head rotation. It is therefore hypothesized that the epaxial and sternohyoideus muscles of a long-snouted syngnathid will either have a larger cross-section or a longer tendon to, respectively, generate extra force and store extra energy for head rotation. In the *Hippocampus* sp. studied, regardless of their snout length, both epaxial and sternohyoideus muscles have a short tendon and a large diameter. On the other hand, the pipefishes studied, with exception of *C. intestinalis*, have slender but very long sternohyoideus and epaxial tendons and muscles. Thus, no trend of either increase or decrease in tendon length or muscle diameter with increasing snout length was observed. Yet, there appears to be a phylogenetic difference (Syngnathinae *v*. Hippocampinae) in head rotation technique. The long tendon and small diameter of the sternohyoideus muscle in the pipefishes seems beneficial for generating the required power. In the *Hippocampus* sp., the large muscle cross-section may indicate that the main force for head rotation is generated by muscle contraction (as opposed to release of stored strain energy). Potentially, the bended neck in the seahorses prevents the optimal functioning of the elastic recoil mechanism in the sternohyoideus and hypaxial muscles as found in pipefishes. *Corythoichthys intestinalis*, however, seems to have an intermediate configuration, with rather short tendon lengths and larger epaxial and sternohyoideus muscles. The similarity with seahorse muscle morphology might be related to their trophic behaviour, sit-and-wait feeding strategy rather than active pursuit of the prey, as in the other pipefishes studied here. Kinematical data of the path travelled by the mouth during feeding also

show a convergence between *Hippocampus* sp. and *C. intestinalis* (Van Wassenbergh *et al*., 2011*b*). Besides that, a recent phylogeny (Teske & Beheregaray, 2009) suggests a closer relationship between *Corythoichthys* and *Hippocampus* species than for instance between the latter and the genus *Syngnathus.* The most recent phylogenetic tree of the Syngnathidae, however, reveals a sister group relationship between *Hippocampus* and *Syngnathus* (Wilson & Orr, 2011).

Apart from the hypothesized differences, some other features are worth mentioning. One of those is the mandibulo-hyoid ligament that encloses the protractor hyoidei muscle entirely, thus forming a sheath for the muscle. This striking configuration is found in both long- and short-snouted pipefishes (*D. dactyliophorus*, *D. pessuliferus* and *C. intestinalis*) and in *H. abdominalis*, but it is absent in the others (*D. janssi*, *D. melanopleura*, *H. reidi* and *H. zosterae*). Hence, it is not related to snout length, neither is it characteristic for pipefishes. The functional advantage of this configuration, however, remains unclear.

An interesting finding related to the epaxial muscle is the presence of a long sesamoid bone embedded into its very firm tendon in all pipefishes studied here (but not in *S. rostellatus*; Leysen *et al*., 2010). Usually, sesamoid bones are formed in tendons that pass over a joint where they protect the tendon from damage and where they could improve the mechanical efficiency of the related muscle (Sarin *et al*., 1999; Hall, 2005). Replacing part of an elastic tendon by a stiff bone seems likely to imply a loss of potential strain energy storage capacity, which would negatively affect the epaxial catapult performance. Potentially, the elastic energy necessary for the power enhancement is stored in the small but firm epaxial ligament connecting the supraoccipital bone with the tendon bone. The fact that this ligament is shorter in the two pipefishes with a short snout (*C. intestinalis* and *D. melanopleura*) supports this hypothesis as less strain energy is probably required for pivot feeding in short-snouted species as the moment of inertia is lower. The epaxial sesamoid bone is found in none of the *Hippocampus* sp. investigated. Again, this might be explained by the seahorse's tilted head, due to which the epaxial tendon is curved and hence the presence of a straight and rigid element within this tendon would probably impede force transfer. More comparative morphological and kinematic analyses will be required before any conclusions can be made on the functional significance on the presence or absence of this sesamoid bone.

A prominent phylogenetic difference in urohyal length was also observed. The seahorses studied here all have a short urohyal bone, with a length of less than the hyoid length and which lacks a bifurcation. In all pipefishes investigated in this study, the urohyal bone is very much elongated with respect to the hyoid length (to even over six times as long in *D. janssi*). The urohyal bone was shortest in *S. rostellatus*, with a length of about twice that of the hyoid (Leysen *et al*., 2010). The urohyal length does not seem to be correlated with snout length as both short- and long-snouted pipefishes have a very long urohyal bone. With the exception of *D. dactyliophorus* and *S. rostellatus*, the pipefish urohyal bone has a bifurcating caudal end, which can be small, as in *C. intestinalis*, or well developed, as in *D. pessuliferus* and *D. melanopleura*, or it can consist of two exceptionally long and slender diverging rods, as in *D. janssi*. Analogous to the epaxial sesamoid bone, the absence of an elongated urohyal in the *Hippocampus* sp. may be related to the tilted position of the head with respect to the body (making the distance along a straight line between the hyoid and the pectoral girdle too short).

In conclusion, some variation in lower jaw rigidity and adductor mandibulae muscle line of action was found between the species, which could be snout length specific. Most striking features, like the mandibulo-hyoid ligament enclosing the protractor hyoidei muscle, the presence of an epaxial sesamoid bone and the elongation of the urohyal bone in some pipefishes or the well-developed sternohyoideus muscle in seahorses, however, could not be explained by variation in snout length. These traits may rather be associated with different force-generating strategies, namely storage and release of elastic energy *v*. pure muscle force.

Research was supported by FWO grant G053907. H.L. is funded by a PhD grant of the Institute for the Promotion of Innovation through Science and Technology in Flanders (IWT-Vlaanderen).

References

Adriaens, D. & Herrel, A. (2009). Functional consequences of extreme morphologies in the craniate trophic system. *Physiological and Biochemical Zoology* **82,** 1–6.

Aerts, P. (1991). Hyoid morphology and movements relative to abducting forces during feeding in *Astatotilapia elegans* (Teleostei: Cichlidae). *Journal of Morphology* **208,** 323–345.

Alexander, R. M. N. & Bennet-Clark, H. C. (1977). Storage of elastic strain energy in muscle and other tissues. *Nature* **265,** 114–117.

Anker, G. C. (1974). Morphology and kinetics of the head of the stickleback, *Gasterosteus aculeatus*. *Transactions of the Zoological Society of London* **32,** 311–416.

Bergert, B. A. & Wainwright, P. C. (1997). Morphology and kinematics of prey capture in the syngnathid fishes *Hippocampus erectus* and *Syngnathus floridae*. *Marine Biology* **127,** 563–570.

Bock, W. J. & Shear, C. R. (1972). A staining method for gross dissection of vertebrate muscles. *Anatomischer Anzeiger* **180,** 222–227.

Branch, G. M. (1966). Contributions to the functional morphology of fishes. Part III. The feeding mechanism of *Syngnathus acus* Linnaeus. *Zoologica Africana* **2,** 69–89.

Gibb, A. C. (1995). Kinematics of prey capture in a flatfish, *Pleuronichthys verticalis*. *Journal of Experimental Biology* **198,** 1173–1183.

Gibb, A. C. (1997). Do flatfish feed like other fishes? A comparative study of percomorph prey-capture kinematics. *Journal of Experimental Biology* **200,** 2841–2859.

Gosline, W. A. (1977). The structure and function of the dermal pectoral girdle in bony fishes with particular reference to ostariophysines. *Journal of Zoology (London)* **183,** 329–338.

Hall, B. K. (2005). *Bones and Cartilage. Developmental and Evolutionary Skeletal Biology.* London: Elsevier Academic Press.

Harrington, R. W. J. (1955). The osteocranium of the American cyprinid fish, *Notropis bifrenatus*, with an annotated synonymy of teleost skull bones. *Copeia* **1955,** 267–290.

Herald, E. S. (1959). From pipefish to seahorse: a study of phylogenetic relationships. *Proceedings of the California Academy of Sciences* **29,** 465–473.

Hunt von Herbing, I., Miyake, T., Hall, B. K. & Boutilier, R. G. (1996). Ontogeny of feeding and respiration in larval Atlantic cod *Gadus morhua* (Teleostei, Gadiformes): II. Function. *Journal of Morphology* **227,** 37–50.

Kendrick, A. J. & Hyndes, G. A. (2005). Variations in the dietary compositions of morphologically diverse syngnathid fishes. *Environmental Biology of Fishes* **72,** 415–427.

Kuiter, R. H. (2003). *Seahorses, Pipefishes and Their Relatives. A Comprehensive Guide to Syngnathiformes.* Chorleywood: TMC Publishing.

Lauder, G. V. (1983). Food capture. In *Fish Biomechanics* (Webb, P. W. & Weihs, D., eds), pp. 280–311. New York, NY: Praeger Publishers.

Lekander, B. (1949). The sensory line system and the canal bones in the head of some Ostariophysi. *Acta Zoologica* **30,** 1–131.

Leysen, H., Jouk, P., Brunain, M., Christiaens, J. & Adriaens, D. (2010). Cranial architecture of tube-snouted Gasterosteiformes (*Syngnathus rostellatus* and *Hippocampus capensis*). *Journal of Morphology* **271,** 255–270.

Lourie, S. A., Vincent, A. C. J. & Hall, H. J. (1999). *Seahorses: An Identification Guide to the World's Species and Their Conservation.* London: Project Seahorse.

Lourie, S. A., Foster, S. J., Cooper, E. W. T. & Vincent, A. C. J. (2004). *A Guide to the Identification of Seahorses.* Washington, DC: Project Seahorse and TRAFFIC North America.

de Lussanet, M. H. E. & Muller, M. (2007). The smaller your mouth, the longer your snout: predicting the snout length of *Syngnathus acus*, *Centriscus scutatus* and other pipette feeders. *Journal of the Royal Society Interface* **4,** 561–573.

Masschaele, B. C., Cnudde, V., Dierick, M., Jacobs, P., Van Hoorebeke, L. & Vlassenbroeck, J. (2007). UGCT: new X-ray radiography and tomography facility. *Nuclear Instruments & Methods in Physics Research A* **580,** 266–269.

Muller, M. (1987). Optimization principles applied to the mechanisms of neurocranium levation and mouth bottom depression in bony fishes (Halecostomi). *Journal of Theoretical Biology* **126,** 343–368.

Muller, M. & Osse, J. W. M. (1984). Hydrodynamics of suction feeding in fish. *Transactions of the Zoological Society of London* **37,** 51–135.

Nelson, J. S. (2006). *Fishes of the World.* Hoboken, NJ: John Wiley & Sons.

Roos, G., Leysen, H., Van Wassenbergh, S., Herrel, A., Jacobs, P., Dierick, M., Aerts, P. & Adriaens, D. (2009*a*). Linking morphology and motion: a test of a four-bar mechanism in seahorses. *Physiological and Biochemical Zoology* **82,** 7–19.

Roos, G., Van Wassenbergh, S., Herrel, A. & Aerts, P. (2009*b*). Kinematics of suction feeding in the seahorse *Hippocampus reidi*. *Journal of Experimental Biology* **212,** 3490–3498.

Roos, G., Van Wassenbergh, S., Aerts, P., Herrel, A. & Adriaens, D. (2011). Effects of snout dimensions on the hydrodynamics of suction feeding in juvenile and adult seahorses. *Journal of Theoretical Biology* **269,** 307–317.

[Correction added after online publication 25 May 2011, reference changed as author order was incorrect]

Ryer, C. H. & Orth, R. J. (1987). Feeding ecology of the northern pipefish, *Syngnathus fuscus*, in a seagrass community of the lower Chesapeake Bay. *Estuaries* **10,** 330–336.

Sarin, V. K., Erickson, G. M., Giori, N. J., Bergman, A. G. & Carter, D. R. (1999). Coincident development of sesamoid bones and clues to their evolution. *Anatomical Record* **257,** 174–180.

Schultze, H. P. (2008). Nomenclature and homologization of cranial bones in actinopterygians. In *Mesozoic Fishes*, Vol. 4, Homology and phylogeny (Arratia, G., Schultze, H. P. & Wilson, M. V. H., eds), pp. 23–48. München: Verlag Dr. Friedrich Pfeil.

Storero, L. P. & González, R. A. (2009). Prey selectivity and trophic behavior of the Patagonian seahorse, *Hippocampus patagonicus*, in captivity. *Journal of the World Aquaculture Society* **40,** 394–401.

Taylor, W. R. & Van Dyke, G. C. (1985). Revised procedures for staining and clearing small fishes and other vertebrates for bone and cartilage study. *Cybium* **9,** 107–119.

Tchernavin, V. V. (1953). *The Feeding Mechanisms of a Deep Sea Fish.* London: British Museum (Natural History).

Teske, P. R. & Beheregaray, L. B. (2009). Evolution of seahorses' upright posture was linked to Oligocene expansion of seagrass habitats. *Biological Letters* **5,** 521–523.

Van Wassenbergh, S., Herrel, A., Adriaens, D. & Aerts, P. (2005). A test of mouth-opening and hyoid-depression mechanisms during prey capture in a catfish using high-speed cineradiography. *Journal of Experimental Biology* **208,** 4627–4639.

Van Wassenbergh, S., Strother, J. A., Flammang, B. E., Ferry-Graham, L. A. & Aerts, P. (2008). Extremely fast prey capture in pipefish is powered by elastic recoil. *Journal of the Royal Society Interface* **5,** 285–296.

Van Wassenbergh, S., Roos, G., Aerts, P., Herrel, A. & Adriaens, D. (2011*a*). Why the long face? A comparative study of feeding kinematics of two pipefishes with different snout lengths. *Journal of Fish Biology* **78**, 1786–1798. doi:10.1111/j.1095-8649.2011.02991.x

Van Wassenbergh, S., Roos, G. & Ferry, L. (2011*b*). An adaptive explanation for the horse-like shape of seahorses. *Nature Communications* **2.**

Vincent, A. C. J. & Sadler, L. M. (1995). Faithful pair bonds in wild seahorses, *Hippocampus whitei*. *Animal Behaviour* **50,** 1557–1569.
Vlassenbroeck, J., Dierick, M., Masschaele, B., Cnudde, V., Van Hoorebeke, L. & Jacobs, P. (2007). Software tools for quantification of X-ray microtomography at the UGCT. *Nuclear Instruments & Methods in Physics Research A* **580,** 442–445.
Westneat, M. W. (1990). Feeding mechanics of teleost fishes (Labridae, Perciformes): a test of four-bar linkage models. *Journal of Morphology* **205,** 269–295.
Wilson, A. B. & Orr, J. W. (2011). The evolutionary origins of syngnathid fishes. *Journal of Fish Biology* **79** (in press).
Wilson, A. B., Vincent, A., Ahnesjö, I. & Meyer, A. (2001). Male pregnancy in seahorses and pipefishes (Family Syngnathidae): rapid diversification of paternal brood pouch morphology inferred from a molecular phylogeny. *Journal of Heredity* **92,** 159–166.
Winterbottom, R. (1974). A descriptive synonymy of the striated muscles of the Teleostei. *Proceedings of the Academy of Natural Sciences of Philadelphia* **125,** 225–317.